Scripta Materialia 60 (2009) 1008–1011
DOI: http://dx.doi.org/10.1016/j.scriptamat.2009.02.040

Influence of yttria additions on the oxidation behaviour of titanium prepared by powder metallurgy

P. Pérez,[a,*] G. Salmi,[b] A. Muñoz[b] and M.A. Monge[b]

[a]*Centro Nacional de Investigaciones Metalúrgicas, CENIM, CSIC, Avda. Gregorio del Amo 8, 28040 Madrid, Spain*
[b] *Universidad Carlos III de Madrid, Dpto. Fı´sica, Avda. Universidad 30, 28911, Spain*

Abstract: The yttria dispersion effect on the oxidation resistance of titanium prepared by powder metallurgy has been evaluated between 700 and 900 °C. Yttria additions slightly increase the oxidation rate up to 800 °C and decrease it considerably at 900 °C. The mul tilayered rutile scale formed on pure titanium prepared by conventional techniques is replaced by a denser rutile scale in the case of titanium prepared by powder metallurgy. Yttria additions raise the temperature at which a more protective dense rutile scale is formed.

Keywords: Powder processing; Yttria addition; Metals and alloys titanium; Oxidation

The use of titanium at high temperatures requires acceptable oxidation behaviour in addition to high strength and good creep resistance. A non-protec-tive multilayered rutile scale grows during long-term exposure of pure titanium in air above 700 °C. This scale, however, cannot prevent oxygen uptake, and accordingly the metal beneath the scale can dissolve sig-nificant amounts of oxygen, which can induce a consid-erable embrittlement of the metal underneath the oxide scale. The oxidation resistance of titanium can be enhanced by adding alloying elements such as Nb [1], Ta [2], A l [3], S i [4] or Cr [5]. The beneficial influence of Nb or Ta arises from the formation of a nitride layer in air which prevents oxygen dissolution in the metal substrate. On the other hand, Al, Si or Cr additions modify the composition and/or structure of the rutile scale, although they are not so effective as Nb or Ta additions. Furthermore, at the concentration levels at which these elements are required to reduce effectively the oxidation rate, second phases can precipitate, producing detrimental effects on the desirable properties of titanium.

In the case of high-temperature Fe-, Ni- and Co-base alloys containing elements which could promote the formation of protective oxide layers such as Cr or Al, fine yttria dispersions contribute to reducing the oxidation rate and enhancing the adhesion of the protective scale [6,7]. Also, the growth mechanism of the oxide scale in these alloys appears to be modified by yttria addition. So far, the effect of yttria additions on the oxidation behaviour of titanium has not been reported.

The aim of the present work was to investigate the influence of yttria additions on the oxidation behaviour of titanium prepared by powder metallurgy (PM) in the temperature range 700 900 °C.

Yttria oxide dispersion strengthened titanium with 0.6 wt.% Y_2O_3 were prepared by a PM route which involves mechanical grinding of Ti and nanosized Y_2O_3 particles, cold isostatic pressing at 250 MPa, sintering in high vacuum at 1300 °C for 4 h, and final hot isostatic pressing (HIP) at 1350 °C for 2 h under a pressure of 200 MPa. The same procedure, apart from the mechanical grinding stage, was used for the processing of PM-Ti. The starting Ti powder had a purity of 98.7% and an average particle size of 8-11 μm and the Y_2O_3 powder had a purity of 99.5% with a particle size below 30 nm. After HIPing, PM-Ti and Ti $0.6Y_2O_3$ had an equiaxial microstructure and a density of 4.47 g.cm ^{3} (99% of theoretical density) and 4.43 g.cm ^{3} (98.2% of theoretical density), respectively. A comparison of the densities measured by the Archimedes method and He-pycnometry showed that both materials contained only closed porosity. The average grain size was 48 ± 5 μm for PM-Ti and 35 ± 4 μm for Ti $0.6Y_2O_3$. Submicron yttria particles were embedded in the titanium matrix,

* Corresponding author. Tel.: +34 915538900; e mail: zubiaur@cenim.csic.es

preferentially located at grain boundaries. The oxygen contents of sintered PM-Ti and Ti $0.6Y_2O_3$ were 0.5 and 0.8 wt.%, respectively.

Disks 10 mm in diameter and 1.7 mm thick were cut and their surfaces were abraded with successively finer silicon carbide papers (up to 1200 grit) and then ultrasonically cleaned with ethanol. Thermogravimetric measurements were conducted in dry air (dewpoint −60 °C) in the temperature range 700 900 °C. Surfaces and cross-sections of the oxidized specimens were studied by scanning electron microscopy (SEM). To prevent scale loss during metallographic preparation, the surfaces were successively coated with a thin gold layer (by sputtering) and a thicker layer of copper (electrolytically deposited). Cross-sections were prepared by conventional metallographic techniques.

Mass gain curves for Ti $0.6Y_2O_3$ and PM-Ti are shown in Figure 1. Mass gain curves were fitted to a power law of the form $\Delta W \quad kt^n$, where ΔW is the mass gain per unit area, k is the oxidation rate constant, n is the rate exponent and t is the exposure time. At 700 °C, the kinetics followed parabolic laws ($n \approx 0.5$) for PM-Ti while they were nearly-parabolic for Ti $0.6Y_2O_3$ ($n \approx 0.7$). At 800 °C, the kinetics obeyed quasi-linear laws ($n \approx 0.8$). At 900 °C, the rapid mass gain during the initial stage slowed down for long-term exposures, with a clear difference between PM-Ti and Ti $0.6Y_2O_3$. For Ti $0.6Y_2O_3$, the initial linear law changed

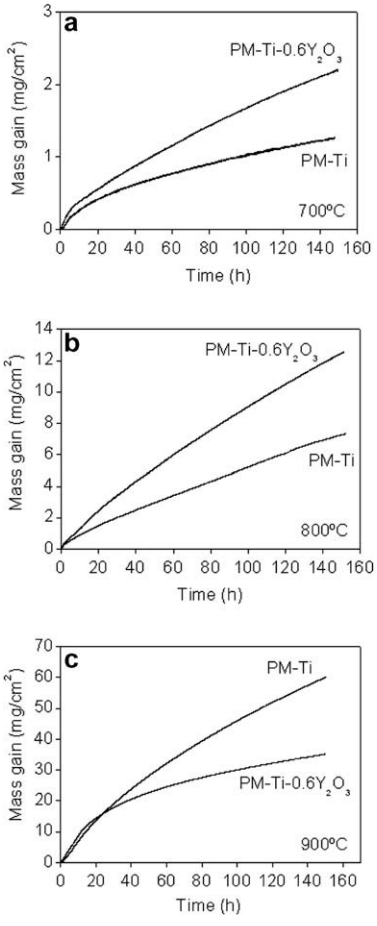

Figure 1. Mass gain curves for PM Ti and Ti $0.6Y_2O_3$ oxidized in dry air at (a) 700 °C, (b) 800 °C and (c) 900 °C.

to parabolic after 15 h of exposure, leading to remarkably slower kinetics, $n \approx 0.5$, whereas in the case of PM-Ti they were quasi-linear for exposures longer than 10 h ($n \approx 0.8$).

Cross-sectional views showed no significant changes in the thickness of the rutile scale at 700 and 800 °C (Fig. 2a d). Thus, after 150 h oxidation at 700 ° C, both materials formed a uniform oxide scale 6 7 μm thick, having a denser layer of about 1 1.5 μm on its outermost surface. After exposure at 800 °C for 150 h, both materials formed a relatively dense scale of about 67 μm thick. Nevertheless, the scale formed on PM-Ti exhibited a multilayered structure, especially in the vicinity the titanium substrate. On the other hand, the scale developed on Ti $0.6Y_2O_3$ contained a significantly lower volume fraction of non-connected porosity and isolated large yttria particles distributed throughout the scale. At both temperatures, major differences between both materials were found inside the metal substrate. Some cracking and small internal rutile islands were found underneath the external scale. These features, especially nodule formation, were absent in metal substrate of PM-Ti.

After 150 h at 900 °C, the scale formed on PM-Ti was much thicker than that formed on Ti $0.6Y_2O_3$, 700 and 165 μm, respectively (see Fig. 2e f). For PM-Ti, rutile layer consisted of a stacking sequence of rutile sub-layers. The thickness of each individual sub-layer was about 3 4 μm. On the other hand, three discernible regions could be distinguished in the scale formed on Ti $0.6Y_2O_3$: (i) a multilayered structure ~40 μm thick at the outermost part of the scale; (ii) a porous layer ~60 μm thick in the central region; and (iii) a relatively dense layer ~65 μm thick adjacent to the scale/metal interface. Isolated intrusions of oxide growing into the metal substrate were found at the oxide scale/metal interface, with some cracks propagating into the metal substrate. These cracks acted as rapid pathways for inward oxygen diffusion, as observed in Figure 3, where cracks interconnecting oxidized zones inside the substrate are observed. Some of these cracks could eventually propagate across the entire sample width, resulting in sample failure. No cracking was observed in PM-Ti.

Mass gain curves proved the slightly detrimental effect of yttria additions on the oxidation resistance of PM-Ti at 700 and 800 °C. On the other hand, ytttria additions were effective at reducing the kinetics at 900 °C. Since the thickness of the external rutile scale was identical for both materials, similar mass gains should be expected. Additional mass gains in Ti $0.6Y_2O_3$ curves arose from the presence of rutile islands inside the Ti matrix. The contribution of this process to the total mass gain tended progressively to be more pronounced as the oxidation temperature increased. It is probable that internal porosity of the material prepared through the PM route caused extensive internal oxidation. Rutile growing on the internal surface of pores at the scale/metal interface should induce stress concentration around them, facilitating nucleation and propagation of microcracks that acted as fast inward diffusion paths for oxygen. If internal porosity or voids were in the crack pathway, oxygen gas could penetrate there, resulting in the extensive formation of oxide nodules,

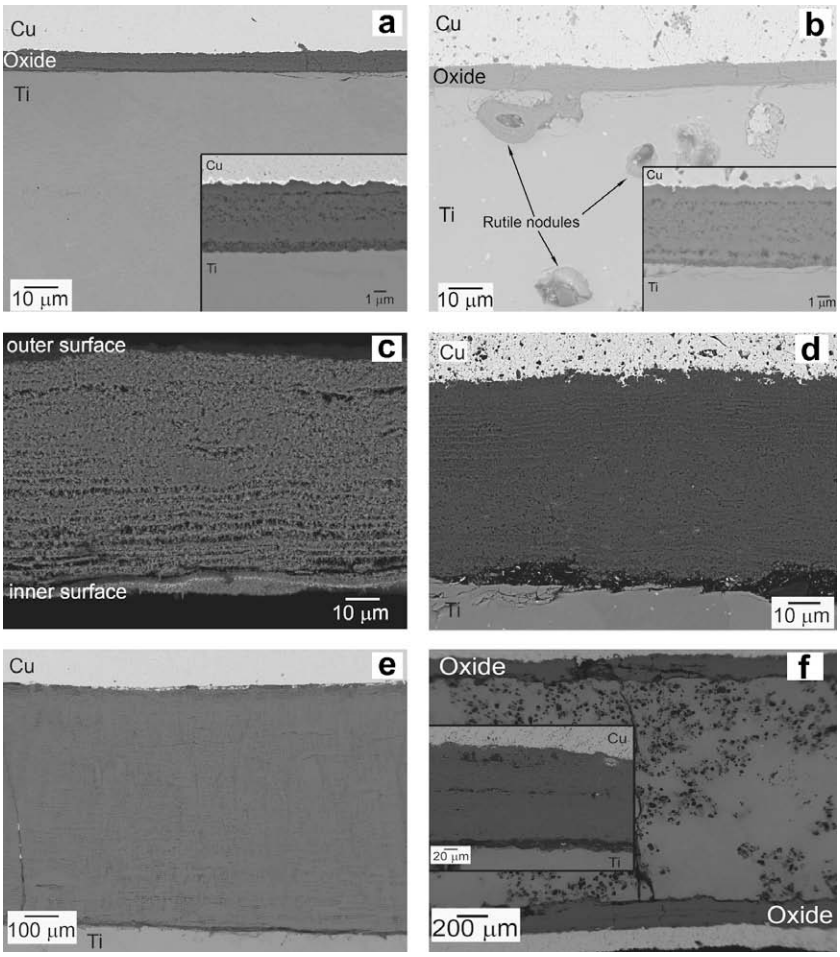

Figure 2. Cross sectional views of the scales formed on PM Ti (a, c, e) and Ti $0.6Y_2O_3$ (b, d, f) after exposure for 150 h in dry air at 700 °C (a, b), 800 °C (c, d) and 900 °C (e, f). Insets show close details of the rutile scale.

especially at 900 °C. Cracking seemed to be associated with yttria additions since no internal oxidation was observed in pure PM-Ti. Yttria particles could act in two ways: (i) preventing good bonding among titanium powders during HIPping; and/or (ii) inducing a significant hardening in the titanium matrix in such a way that rutile growth stresses, generated inside the pores, cannot be plastically released in titanium.

The processing route itself affected beneficially the oxidation behaviour of pure PM-Ti and Ti $0.6Y_2O_3$, as shown in the Arrhenius plot of Figure 4, which shows data regarding oxidation of titanium in several atmospheres in the temperature range 700 900 °C collected from the literature [8 12], as well as parabolic rate constants values calculated in this work for pure PM-Ti and Ti $0.6Y_2O_3$. Parabolic rate constants for both materials prepared by PM, and oxidized in air, were almost one order of magnitude lower over the

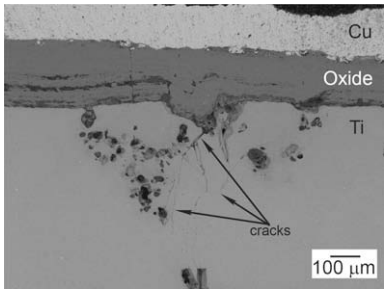

Figure 3. Cracks propagating from a rutile protrusion formed on a void originally present in Ti $0.6Y_2O_3$ after exposure at 900 °C for 150 h.

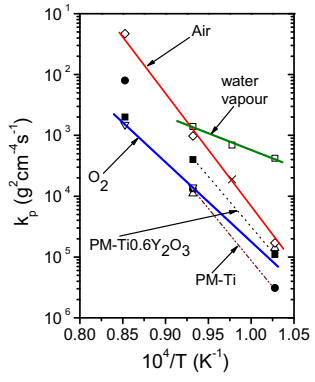

Figure 4. Arrhenius plot of parabolic rate constants (k_p) for PM Ti (●) and Ti $0.6Y_2O_3$ (■). Additional k_p values collected from the literature are: ◇ [1], □ [9], Δ [10, Jenkins data], ▽ [11] and × [12].

entire temperature range than those of as-cast or wrought titanium. Moreover, parabolic rate constants of PM-Ti were comparable or even lower than those of as-cast or wrought titanium oxidized in pure oxygen or water-containing atmospheres. Therefore, the PM route itself induced not only an inherent decrease in the oxidation rate but also changed the structure of the rutile scale. Cross-sectional views proved that the typical multilayered structure of the rutile scale formed at 800 °C in as-cast or wrought titanium [8,10] appeared only at the innermost part of scale. This change in the structure, i.e. in the kinetics, could be attributed to the existence of a thin oxide film covering the original surface of titanium powders which were embedded within the titanium matrix in HIPed material. These fine oxides could hinder periodic fracture of rutile sub-layers, since they could remove rutile growth stresses. Unfortunately, this mechanism was only effective up to 800 °C. If rutile growth rate was very high, growth stresses could not be effectively released from the oxide scale, so the scale developed the non-protective multilayered structure found at 900 ° C (see Fig. 2e). At this temperature, however, yttria additions promoted the formation of a relatively dense rutile layer which reduced considerably the oxi-dation rate.

Activation energies for PM-Ti and Ti $0.6Y_2O_3$ were 324 and 314 kJ mol ^{1}. (Parabolic rate constants at 900 °C were not used for fitting because of the multilayered structure of the scale in PM-Ti. In the case of Ti $0.6Y_2O_3$, the contribution of internal oxidation to the total mass gain at 900 °C was proportionally lower than at 700 and 800 °C.) These values agreed rather well with the activation energy for oxygen diffusion in rutile, 305 314 kJ mol ^{1} [13], so the oxidation mechanism was controlled by inward oxygen diffusion through the rutile scale. It is worth noting that these activation energies were much higher than those of non-PM Ti, 165 200 kJ mol ^{1} [14]. The highest activa-tion energies, about 240 kJ mol ^{1}, were reported for titanium oxidized in Ar/20%O_2 [12]. Such divergences could probably arise from the different structure of the rutile scale relatively dense in PM materials and multilayered in non-PM materials.

The present results reveal the importance of the processing route on the oxidation behaviour of titanium. The use of a PM route caused an inherent decrease in the oxidation rate of titanium and also favoured the formation of a relatively dense rutile scale up to 800 °C. The typical multilayered rutile scale formed on pure titanium prepared by conventional techniques was replaced by a denser rutile scale in the case of PM-Ti. Yttria additions promoted the formation of a dense oxide scale also at 900 °C which contributed to reducing significantly oxidation kinetics in such a way that the typical multilayered structure formed on pure titanium was replaced by a denser oxide scale.

The authors gratefully acknowledge financial support from the Dirección General de Investigación (Ministerio de Ciencia e Innovación of Spain) under grant MAT2006-13005-C03-02, and the Dirección General de Universidades (Comunidad de Madrid) through the program ESTRUMAT-CM (Grant S-0505/MAT/0077).

[1] P. Pérez, V.A.C. Haanappel, M.F. Stroosnijder, Mater. Sci. Eng. A284 (2000) 126.
[2] R.J. Hanrahan Jr., D.P. Butt, Oxid. Met. 48 (1997) 41.
[3] A.M. Chaze, C. Coddet, G. Béranger, J. Less Common. Met. 83 (1982) 49.
[4] A.M. Chaze, C. Coddet, Oxid. Met. 27 (1987) 1.
[5] A.M. Chaze, C. Coddet, Oxid. Met. 21 (1984) 205.
[6] J. Stringer, B.A. Wilcox, R.I. Jaffee, Oxid. Met. 5 (1972) 11.
[7] F.H. Stott, G.C. Wood, J. Stringer, Oxid. Met. 44 (1995) 113.
[8] P. Pérez, Corros. Sci. 49 (2007) 1172.
[9] Y. Wouters, A. Galerie, J.P. Petit, Solid State Ionics 104 (1997) 89.
[10] P. Kofstad, High Temperature Corrosion, Elsevier Applied Science, London, 1988.
[11] M. Simnad, A. Spilners, O. Katz, Trans AIME J. Met. 7 (1955) 645.
[12] Y. Park, D.P. Butt, Oxid. Met. 51 (1999) 383.
[13] P.J. Harrop, J. Mater. Sci. 3 (1968) 206.
[14] J.E. Lopes Gomes, A.M. Huntz, Oxid. Met. 14 (1980) 471.